# PROCEDURES, RESOURCES AND SELECTED RESULTS OF THE DEEP ECLIPTIC SURVEY

M. W. BUIE, R. L. MILLIS and L. H. WASSERMAN
*Lowell Observatory*
*(E-mails: buie@lowell.edu; rlm@lowell.edu; lhw@lowell.edu)*

J. L. ELLIOT
*Massachusetts Institute of Technology and Lowell Observatory*
*(E-mail: jle@mit.edu)*

S. D. KERN and K. B. CLANCY
*Massachusetts Institute of Technology*
*(E-mails: susank@mit.edu; kclancy@mit.edu)*

E. I. CHIANG and A. B. JORDAN
*University of California at Berkeley*
*(E-mails: echiang@astron.berkeley.edu; abjordan@uclink4.berkeley.edu)*

K. J. MEECH
*University of Hawaii*
*(E-mail: meech@ifa.hawaii.edu)*

R. M. WAGNER
*Large Binocular Telescope Observatory*
*(E-mail: rmw@as.arizona.edu)*

D. E. TRILLING
*University of Pennsylvania*
*(E-mail: trilling@astro.upenn.edu)*

**Abstract.** The Deep Ecliptic Survey is a project whose goal is to survey a large area of the near-ecliptic region to a faint limiting magnitude ($R \sim 24$) in search of objects in the outer solar system. We are collecting a large homogeneous data sample from the Kitt Peak Mayall 4-m and Cerro Tololo Blanco 4-m telescopes with the Mosaic prime-focus CCD cameras. Our goal is to collect a sample of 500 objects with good orbits to further our understanding of the dynamical structure of the outer solar system. This survey has been in progress since 1998 and is responsible for 272 designated discoveries as of March 2003. We summarize our techniques, highlight recent results, and describe publically available resources.

## 1. Summary and Goals of the Survey

With the discovery of a large population of objects at or beyond the distance of Neptune comes the ability to learn about the processes that shape our solar system at much greater distances than previously possible. Many groups are focusing on

*Earth, Moon and Planets* **92:** 113–124, 2003.

studying the newly discovered objects themselves through color or spectroscopic measurements, lightcurve and rotation studies, or searches for satellites. However, before these studies can proceed, one must first locate these objects and determine good orbits. Over and above determining existence, having an ensemble of good orbits permits investigations into the dynamical structure of the outer solar system. We wish to understand which objects are likely to be dynamically long-lived and thus may represent undisturbed primordial material. We wish to understand dynamical lifetimes and the role resonances have played over the age of the solar system.

Our project began in 1998 as the first of the large-format CCD mosaic array cameras was commissioned by NOAO at Kitt Peak. Utilizing the Mosaic cameras (0.35 arcmin$^2$, 8k$\times$8k array) at Kitt Peak and Cerro Tololo, we have been pursuing a systematic survey of the near-ecliptic region. In 2001 we were granted 3 years of formal survey status by NOAO which provides 20 nights of access per year (now extended to a fourth year). The goal of the survey is to collect a sample of 500 KBOs with well-established orbits and known observational biases in their discoveries. From this dataset we can address questions of resonance population, inclination distribution, radial distribution, magnitude or size distribution, and more. In this article we present a brief summary of our survey technique, provide a snapshot of our results, and describe resources we have developed for our survey that may be of wider interest to the scientific community.

## 2. Summary of Techniques

### 2.1. Data collection

We have divided the sky up into 12600 field locations whose field centers are within 6.5 degrees of the ecliptic. The abutting fields correspond to the area of the Mosaic array on the sky. Any field (collection of 8 detector images) with one or more stars brighter than $R = 9$ is not used for searching. Also, only those fields that contain 35 or more USNO-A2.0 catalog sources on each CCD are then used for searching. This list contains 1943 total fields at fixed locations that are distributed at all ecliptic longitudes, except for a 20° gap where the ecliptic crosses the galactic plane near the galactic center.

Candidate fields for any given observing run lie within 30° of the opposition point, thus eliminating confusion with the far more numerous main-belt asteroids. We search a field by taking two images on one night separated by between 1.7 and 2.7 hours. We usually attempt a third frame for confirmation on either the preceding or following night. In the early days of the survey, this third frame was not regularly obtained. Foregoing the third frame enabled us to maximize sky coverage and, therefore, the number of objects discovered per night. However, without an observation on a second night, the Minor Planet Center will not announce a discovery

to the community. Because this announcement was judged to significantly increase the likelihood of astrometric observations by others, we began taking third frames of all fields observed in a given run.

All images are binned 2×2 to reduce the readout time and the file size. This produces a final image scale of 0.52 arcsec/pixel which is adequate to sample the seeing disk on all but the best nights. We rarely see signs that the data are undersampled even though sub-arc second seeing is common at these facilities. This situation may well be due to the broad VR filter ($\lambda_{\rm cent} = 6080$ Å, $\lambda_{\rm FWHM} = 2230$ Å) that we use for maximum sensitivity, in that the atmospheric dispersion correction is designed to correct a somewhat narrower bandpass.

### 2.2. DATA PROCESSING

Our data processing pipeline applies simple image processing rules. We subtract overscan and correct for a superbias image on a chip-by-chip basis. Superbias images are generally created from a stack of 10 bias images. Flat fielding comes from taking the first 20–30 images of the night – typically the first set that is collected without a repeated telescope pointing. The data images are combined with sigma-outlier exclusion with a mean of the pixels that do not include sources or cosmic ray hits. While these flats may not represent the best possible calibration products, they are more than adequate to support our source detection procedures.

After the data are flattened, we run a source detection program and generate a list of all sources that are 3-sigma above sky or brighter. Once located, we generate instrumental magnitudes for all sources with the aperture size chosen for that night. Generally we use an aperture of 3 or 4 pixel radius, sometimes as large as 5 on poorer nights.

Following source detection, we solve for an astrometric transformation from pixel coordinates to equatorial celestial coordinates using reference stars from the USNO A2.0 star catalog. The images are strongly distorted, particularly in the corner CCDs, and sometimes determining an astrometric solution can be challenging. All astrometric solutions are visually inspected and verified. A last stage by-product of the astrometric solution is a correspondence between instrumental magnitude and catalog magnitude. We select those stars with consistent PSFs to determine a zero-point correction for each CCD. The process of generating a zero-point correction works very well but the final magnitudes are only as good as the catalog (generally to a few tenths of a magnitude but sometimes much worse, particularly at southern declinations). Work is underway to provide a firm photometric calibration of the survey data.

Given a list of sources with right ascension, declination, and magnitudes for each frame pair, we then compare the two lists and remove all common sources. On the objects left over we look for pairs of objects moving within 30 degrees of the ecliptic with motion rates at or below 5 arcsec/hour. Any such pairs found are tagged for visual confirmation.

The next step in the process is a visual inspection of all image pairs to search for moving objects. We have an IDL-based program that displays the images and allows marking of moving objects. The image pairs are shown with the first epoch in the red image plane and the second epoch in the blue and green image planes. Fixed objects (stars, galaxies, etc.) show as white objects. Moving objects appear as red/cyan pairs that are very easy to spot. This technique is much, much faster than traditional blinking and enables us to quickly identify moving objects. Each image pair is examined successively by two people to minimize the effects of visual fatigue. The first pass is also used to validate any objects found via software. We have tested this method against software detection algorithms and with data salted with synthetic moving objects (Millis et al., 2002). It compares very favorably against all-computer techniques, with essentially no difference in limiting magnitude or completeness except that we can reliably work with pairs of detection images where software-only techniques need three or more frames to be effective. The 50% efficiency detection threshold is quite close to the limiting magnitude of an image, which defined to be the magnitude of a source whose peak pixel is 3-$\sigma$ above sky. Visual inspection does, however, have completely different detection biases from computer techniques, so the final list of objects is more complete than could be obtained from just one technique. Note that in our survey we attempt to mark, measure, and report all moving targets, regardless of rate. Our field size and cadence is such that we are sensitive to motion rates from 0.5 arcsec/hour up to about 200 arcsec/hour.

Once the images have been examined, we compute the right ascension, declination and magnitudes of the moving objects from the previously determined solutions. One person then reviews all slowly moving objects to make a final determination of the validity of the detection and to consult the third image for confirmation (if it exists).

A final review of the candidate objects comes from attempting to fit a family of Väisälä orbits to the observations. If the resulting orbit does not yield a meaningful prograde Kuiper-Belt or Centaur orbit, the object is dropped from the "interesting" object list. The most common reason for rejection in this review is that the positions of the candidate cannot be fit by any physically plausible orbit.

Once these reviews are completed, we compare all measurements against known KBOs and Centaurs to find linkages with already known objects. Once these linkages are identified, all observations are reported to the Minor Planet Center. Generally speaking, completion of the astrometric reference frame determination takes no more than a day or two after the end of the run. In fact, if everything goes well during a run, it is possible to leave the telescope with all the astrometric reductions having been completed. We can often start the visual inspection before the end of the run as well. The rest of the processing can be done in as little as a week following the observing run provided that there are no complications in the data. Normally, the results are available and reported within two to three weeks.

## 3. Summary of Objects Found

Including all overhead we can collect about 110 images per 10 hour night with a 4-minute exposure time. With 3 images per field, this amount yields 37 search fields, or 12.8 square-degrees per night. As of 1 March 2003, we have been allocated 400 hours at Kitt Peak where 244 hours were usable (61%) and 250 hours at Cerro Tololo where 229 hours were usable (92%). To date we have thus surveyed almost 600 square-degrees. Over this region, we have identified 468 interesting objects (moving slower than 15 arcsec/hour within 30 degrees of the opposition point) of which 272 have received official designations.

### 3.1. Special list of "interesting" objects

As the sample size of known KBOs increases, better statistics are realized for mapping out previously known structures (e.g., non-resonant vs. resonant populations). In addition to the routine objects found, we have begun to find the more unusual objects in the outer solar system. In Tables I–IV we provide shorts lists of particularly interesting categories of objects that have well-determined orbits. In each table the object name is given along with the absolute magnitude, $H_V$, semi-major axis, $a$ (in AU), eccentricity $e$, inclination $i$, and perihelion distance, $q$ (in AU). The next column is the uncertainty of the most relevant quantity in each table. Finally, the aphelion distance, $Q$ (in AU), is given followed by the dynamical classification (discussed in the next section). Note that the orbital elements listed and their errors are determined by the method of Bernstein and Khushalani (2000) except that we determine barycentric elements rather than heliocentric elements. Also, the elements are all integrated to a common epoch of 5 August 2003.

Table I shows a list of the intrinsically brightest objects (largest if a constant albedo is assumed). Although this is a short list of objects, there are a wide range of dynamical classes represented here.

TABLE I

Intrinsically bright objects, $H_V < 5$

| Object name | $H_V$ | $a$ | $e$ | $i$ | $q$ | $\sigma_q$ | $Q$ | Type |
|---|---|---|---|---|---|---|---|---|
| (28978) Ixion | 3.2 | 39.4 | 0.243 | 19.7 | 29.8 | 0.006 | 49 | 3:2$e$, 6:4$i^2$ |
| (42301) 2001 $UR_{163}$ | 4.2 | 51.4 | 0.281 | 0.8 | 37.0 | 0.004 | 66 | ScatExtd |
| 2001 $QF_{298}$ | 4.6 | 39.2 | 0.113 | 22.4 | 34.8 | 0.089 | 43 | 3:2$e$ |
| 2001 $UQ_{18}$ | 4.9 | 44.2 | 0.028 | 5.2 | 43.0 | 0.45 | 45 | Classical |
| (19521) Chaos | 4.9 | 45.9 | 0.108 | 12.0 | 41.0 | 0.007 | 51 | Classical |
| 2001 $KA_{77}$ | 4.9 | 47.4 | 0.095 | 11.9 | 42.9 | 0.053 | 52 | Classical |
| 2000 $CN_{105}$ | 4.9 | 44.8 | 0.095 | 3.4 | 40.6 | 0.055 | 49 | Classical |

TABLE II
Distant objects, ($q > 30$, $a > 90$) or ($e > 0.8$)

| Object name | $H_V$ | $a$ | $e$ | $i$ | $q$ | $\sigma_q$ | $Q$ | Type |
|---|---|---|---|---|---|---|---|---|
| 2000 $OO_{67}$ | 9.1 | 523.7 | 0.960 | 20.1 | 20.8 | 0.05 | 1027 | Centaur |
| 2001 $FP_{185}$ | 6.1 | 225.4 | 0.848 | 30.8 | 34.25 | 0.03 | 416 | ScatNear |
| 2000 $OM_{67}$ | 6.3 | 97.3 | 0.597 | 23.4 | 39.19 | 0.03 | 155 | ScatNear |
| 2000 $CR_{105}$ | 6.1 | 229.8 | 0.807 | 22.7 | 44.2 | 0.2 | 415 | ScatExtd |

TABLE III
High-inclination objects, $i > 30$

| Object name | $H_V$ | $a$ | $e$ | $i$ | $q$ | $\sigma_i$ | $Q$ | Type |
|---|---|---|---|---|---|---|---|---|
| 2001 $QC_{298}$ | 5.9 | 46.1 | 0.120 | 30.6 | 40.6 | 0.001 | 52 | ScatNear |
| 2001 $FP_{185}$ | 6.1 | 225.4 | 0.848 | 30.8 | 34.3 | 0.0001 | 416 | ScatNear |
| 2000 $QM_{252}$ | 6.8 | 40.6 | 0.071 | 34.8 | 37.7 | 0.006 | 44 | ScatNear |
| 2002 $XU_{93}$ | 7.9 | 68.5 | 0.695 | 77.8 | 20.9 | 0.058 | 116 | Centaur |

Table II shows a list of the most distant objects: large perihelion distances and large semi-major axes or large eccentricity. The object 2000 $OO_{67}$ has the largest aphelion distance (by a wide margin) of any KBO or Centaur discovered thus far. One object of particular note here (2000 $CR_{105}$) has a perihelion distance well outside the orbit of Neptune (see discussion of Gladman et al., 2002 and Brunini and Melita, 2002). Though its orbit indicates a past scattering event, there are as yet no widely accepted explanations for its origin. Note that all of these objects have moderately large inclinations.

Table III shows a list of the highest inclination objects from our survey. The last object on the table, 2002 $XU_{93}$, has the largest inclination of any object found so far. Only one other object, 2002 $VQ_{94}$ (not found in our survey) has a similar inclination, and both are Centaurs. In the non-Centaur population (including scattered disk), inclinations greater than 35 degrees have not been seen.

Table IV includes all "nearby" objects from our survey. These objects have orbits at or interior to Neptune but beyond Jupiter. Most of these objects are Centaurs but also included is the first known Neptune Trojan object (Chiang et al., 2003a).

### 3.2. Orbit classifications

With the increasing number of objects and the emergence of new dynamical complexities in this sample, we have been forced to revisit the concept of orbit classification. Previous schemes are inadequate to capture the dynamical diversity

TABLE IV
Objects with aphelion at or inside Neptune's orbit, $Q < 35$

| Object name | $H_V$ | $a$ | $e$ | $i$ | $q$ | $\sigma_Q$ | $Q$ | Type |
|---|---|---|---|---|---|---|---|---|
| (54598) 2000 $QC_{243}$ | 7.6 | 16.5 | 0.202 | 20.8 | 13.1 | 0.0007 | 19.8 | Centaur |
| 2000 $CO_{104}$ | 10.0 | 24.3 | 0.152 | 3.1 | 20.6 | 0.009 | 27.9 | Centaur |
| 2002 $PQ_{152}$ | 8.5 | 25.6 | 0.196 | 9.4 | 20.6 | 0.2 | 30.6 | Centaur |
| 2001 $QR_{322}$ | 7.0 | 30.1 | 0.017 | 1.3 | 29.6 | 0.05 | 30.6 | 1:1 |
| 2001 $KF_{77}$ | 9.4 | 26.0 | 0.238 | 4.4 | 19.8 | 0.009 | 32.2 | Centaur |

and similarities in the trans-Neptunian region. Also, attributing membership to a particular resonance has usually relied on an assignment based on semi-major axis, eccentricity, and inclination. Our improved process is discussed at some length in Chiang et al. (2003b) and uses a 3 My forward integration upon which the orbit classification is based. Table V lists the dynamical type for all objects from our survey with observation arcs greater than 30 days. "Qual" is a orbit classification quality code where 3 means that the nominal orbit and its $\pm 3\sigma$ clones agree, 2 means that one clone matches the nominal orbit, 1 means that both clones differ from the nominal orbit, and 0 means that the error was too large to even bother classifying the orbit. The resonant objects are shown with their resonance descriptor of the form M:N which refers to the mean-motion resonance with Neptune, where M is the integer multiplier of Neptune's period and N is the integer multiplier of the object's period. Following the period relationship is listed the form and the order of the resonance. The symbol, $e$ or $i$ refers to the eccentricity or inclination of the object and $e_n$ refers to the eccentricity of Neptune.

## 4. The Outer Edge of the Belt

The size of our sample is now large enough to address the issue of the radial extent of the non-resonant (Classical) belt. We can ask a very simple question of our data: is the outer limit of our sample determined by the limits of our data collection or is it determined by the spatial distribution of the belt? The nominal limiting magnitude for our data is $R = 23.5$. Within our dataset, 38% have a limiting magnitude fainter than 23.5, 44% are between 23.0 and 23.5, 12% are between 22.5 and 23.0, and the final 6% are brighter than 22.5. These limiting magnitudes refer to the brighter limit of the pair of frames used to search each location. When the effects of followup efforts are included, objects with good orbits have a limiting magnitude of roughly $R = 23$. Given the range of $H_V$ seen in the non-resonant population, we should be able to see objects at a greater distance than we do. Additionally, as the heliocentric distance increases the reflex motion of the object

TABLE V
Summary of Object Types Found

| Orbit type | Qual = 3 | Qual = 2 | Qual = 1 | Qual = 0 |
|---|---|---|---|---|
| 1:1 | 1 | 0 | 0 | – |
| 2:1$e$ | 3 | 0 | 0 | – |
| 3:2$e$ | 18 | 6 | 0 | – |
| 3:2$e$+6:4$i^2$ | 1 | 0 | 0 | – |
| 4:3$e$ | 1 | 0 | 0 | – |
| 5:2$e^3$ | 3 | 1 | 0 | – |
| 5:3$e^2$ | 1 | 1 | 0 | – |
| 5:4$e$ | 1 | 0 | 0 | – |
| 7:3$e^4$ | 0 | 1 | 0 | – |
| 7:4$e^3$ | 4 | 3 | 0 | – |
| 8:5$e^3$+8:5$e^2e_n$ | 0 | 1 | 0 | – |
| 9:5$e^4$ | 1 | 1 | 0 | – |
| Centaur | 7 | 2 | 1 | – |
| Classical | 70 | 2 | 0 | – |
| Scattered disk | 24 | 3 | 1 | – |
| Unknown | – | – | – | 59 |

decreases. However, our search strategy can easily discern objects by their motion out to roughly 250 AU, perhaps even further. Our most distant discovery of any dynamical class was an object at 53 AU.

To see if this is a property of our survey or of the non-resonant belt, we took all the non-resonant objects discovered between 41 and 43 AU. Using this sample, we can ask how many of these would be detected at some further distance. In this way we can deduce a relative areal density as a function of heliocentric distance. This curve is shown in Figure 1. Note that the observed relative areal density drops to zero at 50 AU. Using this test, our survey would have seen objects out to 70 AU and this curve would be flat if the areal density were independent of heliocentric distance. The fact that this curve drops to zero is a direct indication of a decrease in the number of objects with increasing distance. This is the so-called "Kuiper Cliff" which has previously been placed at 47 $\pm$ 1 AU by Trujillo and Brown (2001). Our new data are clearly consistent with this prior result. We take Figure 1 as solid evidence that the space density or size-frequency-albedo distribution (or both) of non-resonant objects changes dramatically with heliocentric distance. Our sample is sensitive out to 60–70 AU. For reference, at 55 AU we should have seen 7 objects compared to 28 objects in the observed sample. But, we did not find any classical object beyond 49 AU in our sample.

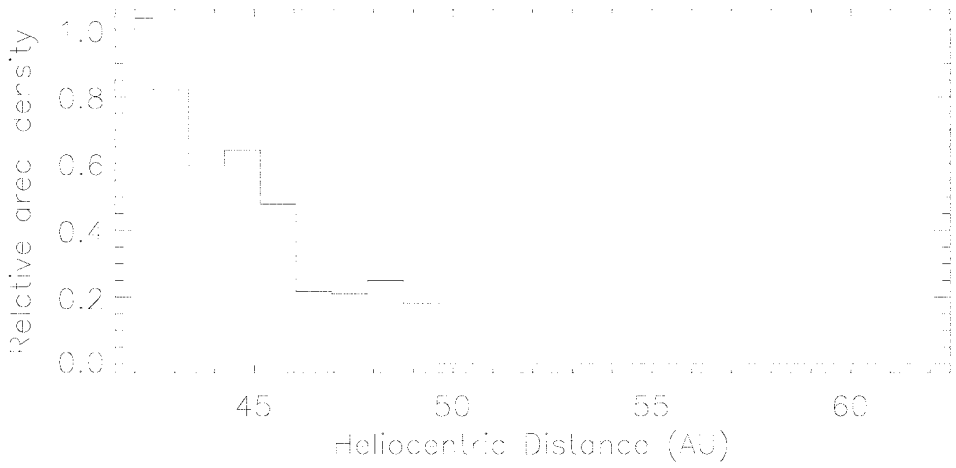


*Figure 1.* Number of non-resonant objects detected relative to the number found at 42 AU. This curve shows the observed fall off in sky density of non-resonant objects as heliocentric distance increases. If the density and size-frequency-albedo distribution were independent of distance, we would have measured $1 \pm 0.4$ at 55 AU.

## 5. Summary of Publically Available Resources

The biggest challenge in reaching the goal of the survey is in obtaining all the followup astrometry needed to secure the orbits of our newly discovered objects. A useful rule-of-thumb for the amount of astrometry needed is 2-2-1, which translates to observations in 2 lunations in the discovery apparition, observations in 2 lunations in the apparition after discovery, and finally one more observation in one lunation in the second year after discovery. In this case, "observation" refers to collecting at least a pair of measurements on a single night. This pattern of observation will usually determine the orbit well enough to establish the dynamical type. Looking at the problem this way, it is clear that discovering objects is only 20% of the work required. It is also true that the power of our wonderful wide-field cameras is wasted on most followup work. We have had to increase the amount of time we spend on followup to the detriment of new discoveries. Only through recovery observations with other telescopes will we reach the goal of 500 secure orbits.

Within the DES team we work aggressively to secure time on other telescopes for followup on Mauna Kea, Lick Observatory, other telescopes on Kitt Peak, Magellan and the Perkins 1.8-m. Despite our best efforts, objects are still being lost, but help from other observers can reduce the loss rate. To facilitate this community-wide collaborative effort we make every effort to release all of our discoveries as soon as possible following a search run. These measurements are all submitted to the Minor Planet Center (MPC), usually within 2–3 weeks after the end of the run. Additionally, we post a considerable amount of information on the

TABLE VI
Summary of public resources

| URL | Content |
|---|---|
| http://www.lowell.edu | Main Lowell Observatory web site |
| /Research/DES/ | Main project summary page with links to other information about the survey. |
| /∼buie/kbo | Main summary of DES objects and observing run status. |
| /kbofollowup.html | Table of links to followup lists. The following links are currently present but their content and organization may change in the future. |
| /nondesig.html | List of our discoveries that are not yet confirmed or designated and with a positional error $< 1°$. This page may also indicate where the next followup attempt will take place. |
| /desig.html | List of all our discoveries that have been designated regardless of their current ephemeris error. This list is similar to but not exactly the same as that generated by the Minor Planet Center. Regardless of formal discovery credit, an object appears here because it can be included as part of the homogeneous dataset from the survey. |
| /table1.html | List of all KBOs and Centaurs with little need of astrometry. This lists DES and non-DES objects. |
| /table2.html | List of all KBOs and Centaurs needing astrometry but whose errors are small. This is a list of objects whose orbits would be improved somewhat by new observations. If you have a small-field instrument, this list would be good to work from but are generally not critical to be observed. |
| /table3.html | List of all KBOs and Centaurs that need astrometry or they will soon be lost. This is the critical list of objects that need observation. Generally their errors are still small enough that they can be found, but if they are not soon observed they will often be lost. |
| /table4.html | List of all KBOs and Centaurs that have very large positional errors and are essentially lost. The ephemeris uncertainties on these objects is generally large enough that a simple pointed recovery effort will not be successful and the object must be re-discovered. |
| ftp://ftp.lowell.edu | |
| /pub/buie/kbo/recov | |
| /YYMMDD.dat | List of all designated KBOs and Centaurs at 0 h UT on the date (YY–year, MM–month, and DD–day) given by the file name. This file contains predicted positions and uncertainties and other information about the astrometry record. This is designed to be used that night in support of recovery observations. |
| /YYMMDD.sdat | List of non-designated objects, same format as .dat files (see `tnorecov.pro` in IDL library). |
| /pub/buie/idl | Repository of all IDL software used in this (and other) projects. |

Lowell Observatory website. Table VI summarizes some of our online resources. The information in these web pages should be mostly self-explanatory. However, take note that wherever an object name appears, it is hyper-linked to a summary of information about that object. The summary includes the output from the orbit fitting process (Bernstein and Khushalani, 2000), all of the astrometry used as input to the fit, and the residuals from the fit. Also note that there will often be astrometry included in our data that are not published by the MPC. We have included all data that we believe are relevant for the object. Most often, the difference comes in partial recovery observations where we have second apparition observations on only one night that we believe constitute a good recovery. However, these observations are not considered an official recovery, and the measurements are not made public by the MPC until another set of observations are collected. These pages are regenerated automatically every morning. It is our hope that by providing these services and promptly reporting our new objects that we enable others to assist with the formidable followup task. We also encourage observers to send us a copy of any data submitted to the MPC in case of any partial recovery observations. If the linkages appear to be valid, the observations will be added to our local database and can be used immediately to guide future recovery efforts.

## Acknowledgements

We thank help from numerous students, including K. Dekker, L. Hutchison, and M. Trimble under the auspices of the NSF and MIT Undergraduate Research Opportunities Programs. This research is based in part upon work supported by the NASA Planetary Astronomy Progam through grants NAG5-8990, NAG5-10444, NAG5-13380, and NAG5-11058; STScI grant GO-9433; and the AAS.

## References

Bernstein, G. and Khushalani, B.: 2000, 'Orbit Fitting and Uncertainties for Kuiper Belt Objects', *Astron. J.* **120**, 3323–3332.

Brunini, A. and Melita, M. D.: 2002, 'The Existence of a Planet Beyond 50 AU and the Orbital Distribution of the Classical Edgeworth-Kuiper-Objects', *Icarus* **160**, 32–43.

Chiang, E. I., Jordan, A. B., Millis, R. L., Buie, M. W., Wasserman, L. H., Elliot, J. L., Kern, S. D., Trilling, D. E., Meech, K. J., and Wagner, R. M.: 2003a, 'Resonance Occupation in the Kuiper Belt: Case Examples of the 5:2 and 1:1 Resonances', *Astron. J.* **126**, 430–443.

Chiang, E. I., Millis, R. L., Buie, M. W., Wasserman, L. H., and Meech, K. J.: 2003b, 'Resonant and Secular Families of the Kuiper Belt' (this volume).

Gladman, B., Holman, M., Grav, T., Kavelaars, J., Nicholson, P., Aksnes, K., and Petit, J.-M.: 2002, 'Evidence for an Extended Scattered Disk', *Icarus* **157**, 269–279.

Millis, R. L., Buie, M. W., Wasserman, L. H., Elliot, J. L., Kern, S. D., and Wagner, R. M.: 2002, 'The Deep Ecliptic Survey: A Search for Kuiper Belt Objects and Centaurs. I. Description of Methods and Initial Results', *Astron. J.* **123**, 2083–2109.

Trujillo, C. A. and Brown, M. E.: 2001, 'The Radial Distribution of the Kuiper Belt', *Ap. J.* **554**, L95–L98.